Building and Environment 44 (2009) 2463–2474

Contents lists available at ScienceDirect

Building and Environment

journal homepage: www.elsevier.com/locate/buildenv

Experimental study of photocatalytic concrete products for air purification

G. Hüsken*, M. Hunger, H.J.H. Brouwers

Department of Civil Engineering, Faculty of Engineering Technology, University of Twente, P.O. Box 217, 7500 AE Enschede, The Netherlands

ARTICLE INFO

Article history:
Received 4 March 2009
Received in revised form
17 April 2009
Accepted 22 April 2009

Keywords:
Air purification
Heterogeneous photocatalysis
Titanium dioxide
Nitrogen oxides
Concrete paving blocks

ABSTRACT

Air quality in inner-city areas is a topic which receives much attention nowadays but in the coming years, the overall interest on this topic will become even bigger. One major concern is caused by the reduction of the limiting values given by the European Council Directive 1999/30/EC [Relating to limit values for sulphur dioxide, nitrogen dioxide and oxides of nitrogen, particulate matter and lead in ambient air. Official Journal of the European Communities 1999, L 163/41–60] and increasing traffic rates especially for diesel powered passenger cars and freight vehicles.

A promising approach for solving the problem of nitrogen oxides (NO_x) is the photochemical conversion of nitrogen oxides to low concentrated nitrates due to heterogeneous photocatalytic oxidation (PCO) using titanium dioxide (TiO_2) as photocatalyst. A variety of products containing TiO_2 are already available on the European market and their working mechanism under laboratory conditions is proven. However, there is still a lack of transforming the experimental results obtained under laboratory conditions to practical applications considering real world conditions.

This paper presents the research conducted on photocatalytic concrete products with respect to the evaluation of air-purifying properties. The degradation process of nitric oxide (NO) under laboratory conditions is studied using a test setup for measuring the performance of photocatalytic active concrete products. The test setup uses the UV-A induced degradation of NO and is oriented on the ISO standard ISO 22197-1:2007. Besides the introduction of the test setup, a uniform measuring procedure is presented to the reader which allows for an evaluation and direct comparison of the performance of photocatalytic active concrete products. This kind of direct comparison was not possible so far. Furthermore, the results of a comparative study on varying photocatalytic concrete products of the European market will be discussed.

1. Introduction

Air pollution caused by road traffic and industry is one of the major problems in metropolitan and urban areas. Despite intensifying emission control requirements (e.g. [5]) and the increased installation of emission reduction systems, the air pollution and in particular the pollution by nitric oxides (NO) from diesel engines will remain a serious issue in the near future (cp. Table 1). The by far largest emissions are generated by local traffic and industrial flue gases (cp. Fig. 1). In this respect, attempts regarding the active reduction of NO can be found in forms of filter devices for industrial stacks (denitrogenization – DENOX plants) or active filter systems for e.g. ventilation outlets of tunnels. According to Matsuda et al. [18], a further solution is the photocatalytic oxidation of nitrogen oxides (NO_x) to low concentrated nitrates. The accruing reaction products in form of nitrate compounds are water soluble and will be flushed from the active concrete surface by rain. The nitrate compounds can be subsequently extracted from the rain water by a standard sewage plant.

When earlier work mainly focused on the treatment of waste water, PCO has received considerable attention regarding the removal of air pollutants during the last years. Since the middle of the 1990s efforts have been made, first in Japan, in large scale applications of this photocatalytic reaction for air-purifying purposes and self-cleaning applications. The construction industry provides several products containing photocatalytic materials since the middle of the 1990s on commercial basis. These products are for example window glass and ceramic tiles providing self-cleaning features. The utilization of the self-cleaning abilities of modified blends of cement was used for the first time in 1998 for the construction of the church "Dives in Misericordia" in Rome.

For the degradation of exhaust gases originated from traffic, a sheet-like application close to the source is desirable. Suitable surfaces for applications which are close to the source of the

* Corresponding author.
E-mail address: g.husken@ctw.utwente.nl (G. Hüsken).

0360-1323/$ – see front matter © 2009 Elsevier Ltd. All rights reserved.
doi:10.1016/j.buildenv.2009.04.010

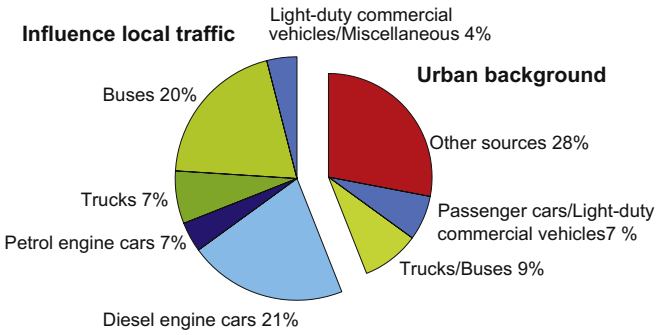

Fig. 1. NO_2-concentration and sources at the traffic site "Stuttgart-Mitte" [15].

emission can be found in large illuminated surfaces in the direct road environment. These are for example noise barrier walls and the road or sidewalk surfaces itself. The production of the first concrete paving blocks specially designed for the degradation of exhaust gases started in 1997 in Japan. In 2002, investigations to the application of a cement based asphalt slurry seal have been conducted in Italy.

Titanium dioxide (TiO_2) in low concentration is applied as photocatalyst for the photocatalytic oxidation process. This photocatalyst appears to be the most suitable semiconducting material and is making use of the UV-A part of the sunlight for the chemical conversion of NO_x. TiO_2 is one of the oxides of titanium, also called rutile titanium white. It appears in remarkable extent in nature – the ninth most abundant element in the earth's crust. In solid state, TiO_2 can appear in three different crystalline modifications namely: rutile (tetragonal), anatase (tetragonal) and the seldom brookite (orthorhombic). However, only the optoelectronic properties of the anatase modification turn this crystalline modification to the best suitable photocatalytic material. On the one hand, the semiconductor band gap E_g of 3.2 eV is wide and on the other hand the oxidizing potential of the valence band is with 3.1 eV (at $pH = 0$) relatively high. Both facts lead to the conclusion that multitude of organic and inorganic molecules can be oxidized in the presence of TiO_2 and UV-A light. This also applies for low oxidizable molecules. Besides the high photocatalytic efficiency of TiO_2 due to its material properties, anatase is suitable for the photocatalytic degradation process because it is chemically stable, harmless and, compared to other semiconductor metal oxides, relatively cheap.

The PCO is induced by the transfer of electrons from the valence band to the conduction band by photons in the UV-A range. The UV-A absorption creates electron holes which are responsible for the formation of radicals and charged species such as $OH^{\bullet}$, $O_2^{\bullet -}$, $HO_2^{\bullet}$. The generation of hydroxyl radicals results from the presence of water at the surface of the photocatalyst. For this purpose, a certain amount of water molecules, supplied by the relative humidity, and electromagnetic radiation is required to start the degradation process. The electromagnetic radiation E is expressed by the product of Planck's constant h and the frequency f [9]:

$$TiO_2 \xrightarrow{hf} TiO_2 + e^- + h^+ \quad (1)$$

$$H_2O \leftrightarrow OH^- + H^+ \quad (2)$$

$$OH^- + h^+ \rightarrow OH^{\bullet} \quad (3)$$

The formed hydroxyl radicals act as a strong oxidant for organic and inorganic compounds in further reactions. According to Herrmann et al. [9], the most reactive species are hydroxyl radicals which are the best oxidizing species after fluorine. The further reactions are being subject to the heterogeneous photocatalysis and characterized by the adsorption of the precursor and the desorption of the reaction products.

In this paper, a setup and a measuring procedure for the evaluation of photocatalytic concrete products is described and employed. Using this setup, the effect of influencing parameters on the degradation of NO is studied and an appropriate measuring procedure for the direct comparison of photocatalytic concrete products is presented. The suggested measuring procedure was used for the assessment of photocatalytic concrete products which render a representative overview of the European market.

2. Measuring principle

The PCO is capable of degrading a broad range of pollutants, both of organic and inorganic nature. Therefore, a number of substances are suitable for the assessment of a system's photocatalytic efficiency. Literature shows that the broad field of model pollutants and respective test procedures can be sub-classified into three categories according to the materials used for analysis, namely:

- Dyestuffs (e.g. [23,17]),
- Organic compounds like volatile organic compounds[1] (VOCs) [27],
- Inorganic gases (e.g. [26,6]).

Dyes are degraded by TiO_2 under the influence of UV or solar light. The decomposition is assessed by decolorization measurements (color removal ratio) as well as chromatographic investigations. This widespread application of, for example, methylene blue and Rhodamine B originates from the mainly nontoxic and convenient use of these dyes. However, the decomposition process of dyes is still subject of discussion as these substances only show a limited resistance to UV light, independent of the existence of a catalyst. Stephan et al. [24] for example refer to a 30% degradation of methylene blue within a 4 h UV exposure in the absence of any catalyst.

As methylene blue is also an indicator for redox reactions, it can be decolorized by the reduction reaction as well. As this reaction is invertible, the reduced methylene blue can also be oxidized again and obtain its original color. Therefore, the decolorization is not an unambiguous criteria for the complete degradation of a dye. Since dyes show no absolute resistance to UV induced degradation and decolorization by other substances, they appear not to be an ideal model pollutant.

Furthermore, VOCs are prominent representatives for modeling the degradation of polluted air for indoor situations. Common used organic compounds are:

- Trichloroethylene (C_2HCl_3) [14]
- Acetone (C_3H_6O), 1-butanol ($C_4H_{10}O$), butyraldehyde (C_4H_8O) and *m*-xylene (C_8H_{10}) [22]
- 1,3-Butadiene (C_4H_6), toluene ($C_6H_5CH_3$) [20]
- Formaldehyde (CH_2O) [20,22].

PCO can decompose VOCs to harmless substances like CO_2 and H_2O. This also includes the removal of odors, which makes PCO especially attractive for treating air in house venting systems.

[1] In this paper, volatile organic compounds (VOCs) mean all organic compounds arising from human activities, other than methane, which are capable of producing photochemical oxidants by reactions with nitrogen oxides in the presence of sunlight [7].

As this research is focused on the photocatalytic properties of concrete, in particular on paving blocks, VOCs do not turn out to be representative pollutants for the modeling of outside conditions. Furthermore, many of these model pollutants, like for example formaldehyde, are toxic or generate harmful byproducts which make them difficult to handle. Moreover, during the degradation, CO_2 is produced as one of the major reaction products. Considering the tendency of concrete to carbonation, part of these reaction products can be already transferred to solid $CaCO_3$ in the outer pore system. Therewith, a part of the reaction products mineralize and a quantitative assessment is hampered as the amount of mineralized CO_2 consumed by the carbonation is difficult to assess.

From the facts above, it can be concluded that the application of dyes, VOCs and aromatic compounds is less suitable for the PCO of concrete substrates under outdoor exposition. With regard to acid rain, one of the most serious environmental problems across the world, NO_x seems to be a suitable model pollutant for the assessment of photocatalytic concrete products and their modeling. NO_x and sulphur dioxide SO_2 do not only pose a threat to human health and the preservation of nature, but they are also causing degradation to many inner-city buildings [6]. A large part of the NO_x in the atmosphere has been emitted by car traffic and transport. Therefore, the application of a photocatalytic paving block 'close to the source of emission' is a desirable solution. Considering the before mentioned facts, NO has been selected as model pollutant and a standard measuring procedure was defined which will be explained.

From the relevant literature (e.g. [26,6]) it becomes clear that the degradation of NO or more generally of NO_x, also referred to as the DeNOx-process (denitrogenization), delivers a suitable model to assess the ability of surfaces for air purification. This denitrogenization process can roughly be described as a two-stage reaction on the surface of the photocatalyst:

$$NO + OH^{\bullet} \rightarrow NO_2 + H^+ \quad (4)$$

$$NO_2 + OH^{\bullet} \rightarrow NO_3^- + H^+ \quad (5)$$

The free hydroxyl radicals $OH^{\bullet}$ originate on the anatase surface in presence of water and the therewith connected water electrolysis. As mentioned before, the $OH^{\bullet}$ act as a strong oxidant and oxidize NO to NO_2 in the first step. The formed NO_2 is a key precursor for the further reaction and is oxidized to nitrate ions (NO_3^-) which can either be bound by alkalies dissolved in the pore solution or will, most probably, be flushed from the concrete surface as weak nitric acid. These two reactions describe the processes on the surface of the sample and therefore define the compounds which have to be measured. The quantitative analysis of the reaction products considering the initial pollutant concentration allows evaluating the degradation ability. Furthermore, considering varying flow conditions as well as process conditions allows the modeling of the degradation process. With the help of a chemiluminescence NO_x analyzer, the amount of NO, NO_2 and NO_x can be quantified.

The chemiluminescence is the emission of non-thermal light in the range from 560 to 1250 nm when NO_2 in its excited state changes to the de-excitation state (operation manual Horiba APNA-370 [11]). This reaction takes places, if NO/NO_2 in the sample gas reacts with ozone (O_3). During this reaction, the NO is partly oxidized by O_3 to become NO_2. Part of the NO generated is in the excited state and radiates light when it changes to the ground state.

$$NO + O_3 \rightarrow NO_2^* + O_2 \quad (6)$$

$$NO_2^* \rightarrow NO_2 + hf \quad (7)$$

This reaction proceeds fast and only NO is involved. Therefore, the NO_x analyzer separates the sample gas into two lines. In one line, NO_2 is reduced to NO by the NO_x converter and used as sample gas for measuring the NO_x concentration. The remaining line uses the NO sample gas as it is. The required O_3 of the oxidation process is supplied by the ozone generator using dried ambient air. The O_3 is conveyed into the reaction chamber where also the sample gases are fed in alternating sequence by solenoid-controlled valves. In the reaction chamber, the O_3 reacts with the sample gasses and the emitted light is detected by a photodiode with upstream optical filters. The output of the photodiode is proportional to the concentration of NO and NO_x. Evaluation electronics enables the output of the concentration of NO, NO_2 and NO_x as continuous signal which can be recorded during the measurement.

3. Test setup

The conduction of comparable and repeatable measurements requires the use of an appropriate test setup as well as a reliable measuring procedure. Therefore, a setup for measuring the performance of photocatalytic active concrete products was designed. The test setup uses the UV-A induced degradation of NO and is oriented on the standard ISO 22197-1:2007. This standard holds for advanced technical fine ceramics but it satisfies the needs for measurements on concrete specimen as well. Therefore, the recommendations given by the standard are largely followed for the measurements and scaled according to the requirements on photocatalytic concrete products. The applied test setup is schematically depicted in Fig. 2 and consists of:

- A reactor cell housing the sample
- A suitable UV-A light source
- A NO_x analyzer and
- An appropriate gas supply.

3.1. Reactor cell

The core of the experimental setup used is a gas reactor allowing a planar sample of the size $100 \times 200\ mm^2$ to be embedded. The schematic representation of the reactor cell is given in Fig. 3. The reactor is made from materials which are non-absorbing to the applied pollutant and can withstand UV-A light of high irradiance. On top, the reactor is tightly closed with a glass plate made from borosilicate glass allowing the UV-A radiation to pass through with almost no resistance. Within the reactor the planar surface of the specimen is fixed parallel to the covering glass, leaving a slit H of 3 mm for the gas to pass through. The active sample area used for the degradation process is, deviating from the ISO standard, enlarged from 49.5 mm ± 0.5 mm in width and 99.5 mm ± 0.5 mm in length to $B = 100$ mm and $L = 200$ mm (with similar tolerance), which better complies with standard paving block dimensions. By means of profiles and seals, the sample gas only passes the reactor through the slit between the sample surface and the glass cover in longitudinal direction. All structural parts inside the box are designed to enable laminar flow of the gas along the sample surface and to prevent turbulences.

3.2. Light source

The market for TiO_2 offers a number of varying photocatalytic powders which are available as doped and undoped powders. The application of undoped TiO_2 requires the use of UV-A light as the cut-off wavelength of conventional TiO_2 is 388 nm [2]. Therefore, the spectrum of the light source has to be adjusted according to the cut-off wavelength of the applied powder. This fact was considered

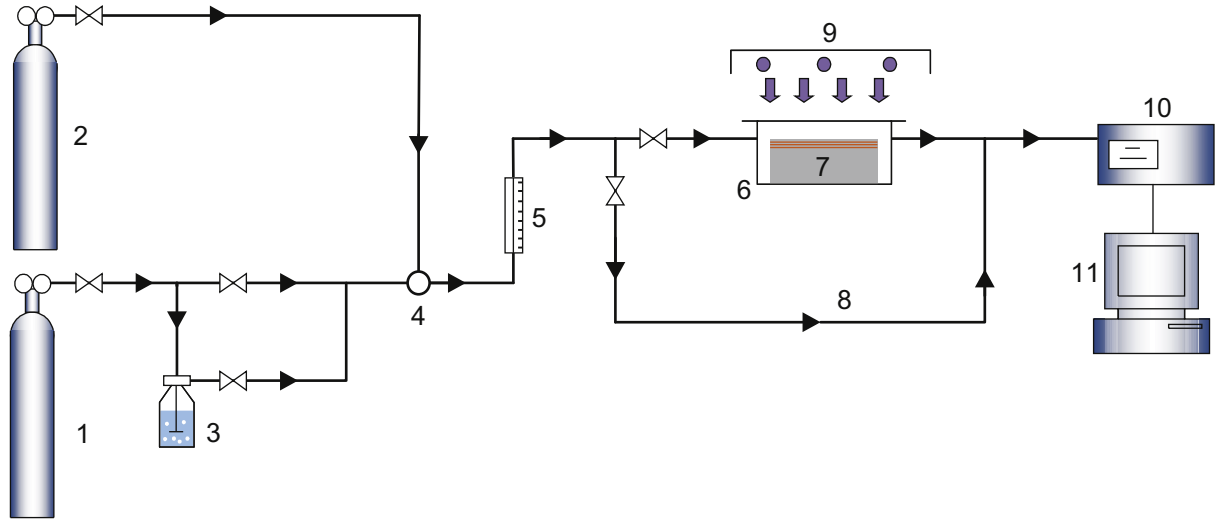

Fig. 2. Schematic diagram of the test setup. 1 Synthetic air. 2 NO source. 3 Gas-washing bottle. 4 Temperature and relative humidity sensor. 5 Flow controller. 6 Reactor cell. 7 Paving block. 8 Side stream for bridged flow. 9 Light source. 10 NO_x analyzer. 11 Computer.

during the development of the test setup which furthermore allows a quick replacement of the light source.

Two light sources with different peaks in their spectrum are available. These are i) a UV-A light source for tests on undoped powders in the anatase modification and ii) a light source using standard fluorescent lamps for doped powders having a broader spectrum covering also the visible light spectrum.

The applied light source is composed of three fluorescent tubes of 25 W each, emitting a high-concentrated UV-A radiation in the range of 300–400 nm with maximum intensity at about 345 nm. Due to the narrow range in wavelength, an addition of a filter was not necessary. The standard fluorescent lamps of 18 W each emit cool day light in the range of 420–650 nm with three prominent peaks at 460, 560 and 600 nm.

A warming of the reactor by the light source is prevented by the spatial separation of light source and reactor and a cooling of the lamps by means of fans. All fluorescent tubes can be adjusted in their irradiance via a dimmer. Therefore, the irradiance can be adjusted exactly to 10 W/m^2 at the sample surface for the use of UV-A irradiation with the help of a calibrated UV-A radiometer. For adjusting the light source using conventional fluorescent light tubes, two different types of sensors are available. The available sensors of the radiometer measure i) the irradiance for blue-green light in the range of 400–480 nm (VIS-BG) or ii) the illuminance according to the day sensitivity curve of the eye in the range of 440–650 nm (VIS-L). The sensors are equipped with an integrated diffusor for the cosine correction that is necessary at non-perpendicular irradiation.

A lead time of about 15 min has to be considered for fluorescent tubes to obtain a stable UV-A radiation is approached.

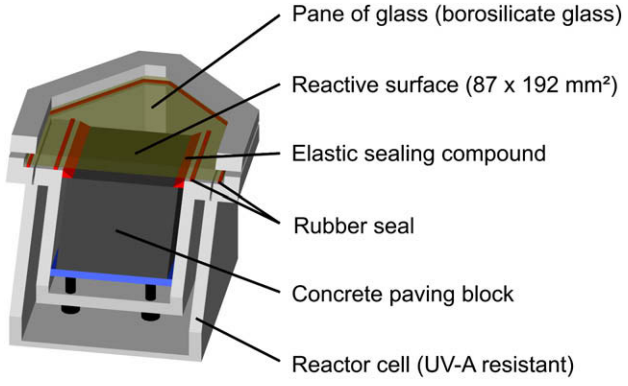

Fig. 3. Schematic diagram of the reactor cell.

3.3. Gas supply and test gases

As already discussed in Section 2, NO was chosen as model pollutant for conducting the experiments on photocatalytic concrete products. According to the requirements given in the standard ISO 22197-1:2007 [12], the concentration of NO in the gas inlet of the reactor has to be 1 ppmv. Therefore, the model pollutant is mixed with an inert transport fluid in order to obtain the desired concentration and flow rate. In this case, the model contaminant composed of 50 ppmv NO, stabilized in nitrogen (N_2), is mixed with the transport fluid. As transport fluid, synthetic air being composed of 20.5 vol.-% of oxygen (O_2) and 79.5 vol-% of nitrogen (N_2) is deployed. Since the gas is delivered in gas cylinders under high pressure, the gas needs to pass a pressure reducing valve before entering the system. Here, pressure is first reduced to 0.3 bar.

Before the two gas flows are merged, the model contaminant has to pass a high precision valve in order to adjust the concentration of the model pollutant to 1 ppmv NO. While adjusting the NO concentration to the desired value, the reactor cell can be bridged by a bypass in the system in order to avoid a premature pollution of the samples surface by NO. During the adjustment of the system, the NO concentration is monitored by the NO analyzer, connected to the outlet of the gas supply unit.

Table 1
Exceeding of the limiting values of the Council Directive 1999/30/EC for the Netherlands (VROM [25]).

	Emission [kiloton]				
	1990	2000	2010	NEC ceiling	Exceeding
SO_2 (NEC)	18	10	4	4	0
NO_x (NEC)	355	280	185	158	27
NH_3 (NEC)	1	3	3	3	0
NMVOS (NEC)	198	114	55	55	0
PM10	26	20	14		
NO_x maritime shipping	20	24	30		
SO_2 maritime shipping	12	14	9		

Furthermore, an adjustable part of the synthetic air is conveyed through a gas-washing bottle, filled with demineralized water, in order to keep the relative humidity of the supplied gas constant at 50%. This is realized by using a split gas flow having a dry and humidified line adjusted by a further metering valve. Behind this stage both gas flows, pollutant and transport fluid, are mixed. With the help of a flow controller, a volume flow of $Q = 3$ l/min is adjusted which corresponds to a flow velocity v of 0.17 m/s along the samples surface considering the geometric dimensions of this section. The Reynolds number of the flow reads:

$$Re = \frac{v_{\mathrm{air}} D_{\mathrm{h}} \rho_{\mathrm{air}}}{\mu_{\mathrm{air}}} = \frac{2 v_{\mathrm{air}} H \rho_{\mathrm{air}}}{\mu_{\mathrm{air}}} = \frac{2Q}{B v_{\mathrm{air}}} \tag{8}$$

D_{h} is the hydraulic diameter of the considered channel, defined as four times the cross-sectional area divided by the perimeter. For the slit considered here, $D_{\mathrm{h}} = 2H$. Substituting $Q = 3$ l/min, $B = 100$ mm and $\upsilon_{\mathrm{air}} = 1.54 \times 10^{-5}$ m^2/s (1 bar, 20 °C) yields $Re \approx 65$. This low Reynolds number implies that the flow within the reactor cell is laminar. A fully developed parabolic velocity profile will be developed at $L_{\mathrm{d}} = 0.1 \mathrm{ReH}$, so here $L_{\mathrm{d}} \approx 20$ mm [3]. That means that only the first 10% of the slit length is influenced by entrance effects. In the remaining 90% of the reactor cell prevails a fully developed laminar flow profile.

The gas, mixed and humidified this way, enters the reactor and is conveyed along the illuminated sample surface. At the opposite site of the reactor the gas leaves the chamber and is transported to a flue or outside with the help of an exhaust air duct. The NO_x analyzer samples the reacted test gas from the exhaust line. An adequate dimensioning of the hose line and, possibly, the installation of non-return valves prevents from sucking leak air from outside via the hose line to the analyzer.

3.4. Analyzer

For the gas analysis, a chemiluminescent NO_x analyzer as described in ISO 7996:1985 [13] is used. The analyzer measures the NO_2 and NO concentration in steps of 5 s while the corresponding NO_x concentration is computed by the difference of the previous two. During the measurement, the analyzer is constantly sampling gas with a rate of 0.8 l/min. The detection limit of the deployed analyzer is at about 0.5 ppbv.

4. Evaluation of measurements

For the sake of repeatability and accuracy, a defined measuring procedure using constant experimental conditions is necessary. Therefore, a measuring procedure has been established which is based on the experience obtained by several measurements carried out during the development phase.

4.1. Measuring procedure

The principle of the conducted measurements is illustrated in Fig. 4. This procedure distinguishes a bridged and non-bridged flow and allows therefore for a much shorter period of adjusting the volumetric flow, pollutant, concentration and humidity. When a stable pollutant concentration has been achieved the bridge will be closed and the gas will flow along the surface of the concrete sample. Now, the pollutant concentration will decrease since the air containing no NO in the reactor cell has to be exchanged and adsorption of NO will take place at the sample surface. At a certain moment, the surface is saturated and the NO concentration returns to the primary inlet concentration. Area and amplitude of this adsorption curve has been shown to be strongly influenced by the surface texture of the sample.

For standard flow conditions ($Q = 3$ l/min, $C_{\mathrm{g,in}} = 1$ ppmv), a period of five minutes is adequate to obtain the primary inlet concentration again. At this moment, the sample is exposed to UV-A light for the case of undoped TiO_2 or any other type of irradiation in the case of doped TiO_2. This leads to an immediate decrease in the NO concentration. This process of active degradation is conducted for 30 min. At the end, the light source will be switched off and the NO concentration ideally returns to the original inlet concentration. Here, also a period of five minutes turned out to be sufficient as the degradation of NO is not stopped immediately after switching off the light source. The reason for this is explained by the inertia of the system. As a matter of principle, no conversion can take place after removing the light source but already formed hydroxyl radicals and charged species can still start an oxidation. This process will last till these substances are consumed by NO and NO_2 molecules. For this reason, the terminal degradation of NO and NO_2 without light exposure is not further assessed.

If not mentioned otherwise, the experimental parameters of the setup are oriented on the requirements given in the standard ISO 22197-1:2007. The following parameters are used for conducting the measurements:

Pollutant concentration (NO): 1.0 ppmv
Flow rate Q: 3.0 l/min
UV-A irradiance: 10.0 W/m^2
Relative humidity: 50%.

4.2. Evaluation of the measurements

All samples that have been tested were subjected to the measuring procedure described before. The further interpretation of the measuring data is conducted following a three stage analysis. For this purpose, the course of the NO conversion is assessed for a time range of five minutes equally distributed over the total measuring period. Fig. 4 illustrates this procedure for the degradation of NO with an arbitrary sample. The degradation rate $\mathrm{Deg_{beg}}$ [%] in the assessed time range is calculated by means of the ratio between actual conversion $\mathrm{Con_{beg}}$ and the total possible conversion of NO $\mathrm{Con_{tot}}$ as follows:

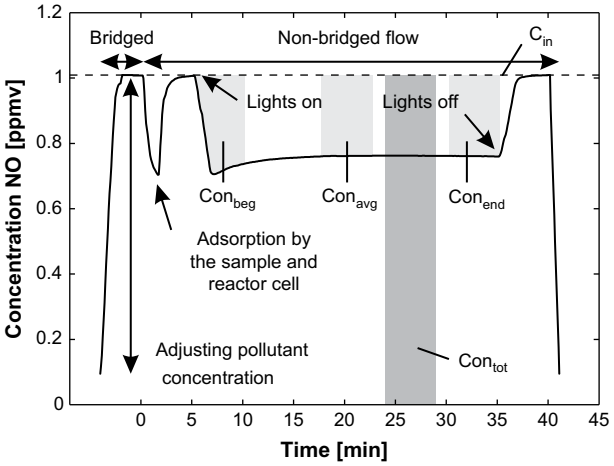

Fig. 4. Sequence of a standard measurement and basic scheme of the data analysis.

$$\mathrm{Deg}_{\mathrm{beg}} = \frac{\mathrm{Con}_{\mathrm{beg}}}{\mathrm{Con}_{\mathrm{tot}}}100 \tag{9}$$

The actual conversion for each 5 min period used in Equation [9] was determined by integrating the associated, descriptive function in the limits of time by using the trapezoid rule:

$$\mathrm{Con}_{\mathrm{beg}} = \sum_{i=1}^{n} \frac{t_{i+1} - t_i}{2}(C_i + C_{i+1}) \quad \forall t_i \in \left[t_{\mathrm{beg}}, t_{\mathrm{beg}} + 5\ \mathrm{min}\right] \tag{10}$$

This approach can be assumed to be sufficiently precise, given that the interval $[t_i, t_{i+1}]$ only lasts for 5 s. Here, the first time interval for the beginning conversion $\mathrm{Con}_{\mathrm{beg}}$ starts at 5 min, when the sample within the reactor was exposed to the radiation for the first time and lasted for 5 min. Using this approach, the slope of the starting conversion up to the maximum degradation rate is included and therefore characterizing this first numerical value.

In other words, the progress of the degradation development up to the maximum conversion is included and evaluated. The second time frame represents the conversion after half of the total time of light exposure, the so-called average conversion $\mathrm{Con}_{\mathrm{avg}}$. The average conversion is characterized by the chronological middle of the measurement ± 2.5 min. For the last time interval, the conversion at the end of the measurement $\mathrm{Con}_{\mathrm{end}}$ is determined. For that purpose, the last 5 min before switching off the light source are considered in order to avoid the influence of the delayed decrease of the conversion after the obvious inflection point.

5. Experimental observations

5.1. Comparative study

The application of TiO_2 in concrete paving blocks is patent-protected for the European market by Murata et al. [19] (Mitsubishi Materials Corporation) as well as Cassar et al. [4] (Italcementi S.p.A.). The patent owned by Mitsubishi Materials Corporation comprises the application of TiO_2 in a functional surface layer of a double-layer paving block having enhanced NO_x-cleaning capability. The thickness, porosity as well as the surface texture of the surface layer is claimed by the patent. Furthermore, the patent claims the concentration of TiO_2, use of appropriate aggregates having a high NO_x adsorption rate, or high light transmission properties.

The patent held by Italcementi S.p.A. covers the application of suitable photocatalytic particles (most preferable TiO_2) in paving tiles capable to oxidize polluting substances present in the environment. The patent describes the application of the photocatalytic material in mass with respect to the amount of cement or binder used. Furthermore, the patent claims the composition of a dry premix containing a hydraulic binder and a TiO_2 based photocatalyst capable of oxidizing organic and inorganic pollutants to maintain the original brilliance and color quantity. For a better understanding, a tabular comparison of both patents is given in Table 2.

Regarding the current market situation, a wide variety of cement based products containing TiO_2 can be found for horizontal and vertical application. Based on the patents owned by Mitsubishi Materials Corporation and Italcementi S.p.A., products having different properties are available on the European market. These products show varying amounts of TiO_2, having preferably the active anatase structure, but also the application of blends of titanium dioxide having anatase and rutile structure is comprised in the patents. These products are promoted regarding their photocatalytic capabilities under laboratory conditions. A comparative assessment in terms of the efficiency of different products has not been carried out so far. There is no doubt about the working mechanisms of the photocatalytic reaction under laboratory conditions but there are still questions open relating to the efficiency of different products. The comparison of different products is rather difficult as different test procedures are used by the manufacturers. These test procedures differ in their execution and therefore a comparison of different products is questionable. Hence, a representative profile of economically available products of the European market is considered and tested using the test procedure described in Section 4.

5.1.1. Sample description

For the comparison, the concrete product industry was requested for appropriate samples. Most of the received samples can be assigned to the paving stone industry. Other samples providing an air-purifying ability have been tested in addition. It is assumed that this survey covers the main part of the European market on the production of concrete elements providing NO_x degradation abilities. In Table 3 the denomination and description of the tested samples is given.

The sample series D_1, D_2, D_3 and D_5 all represent paving stones of different producers. These stones are produced in double-layer technique having an economically priced core mix and a high-quality top layer containing the photocatalyst and satisfying all esthetic requirements. Whereas the stones from series D_3 and D_5 have been taken from the production. Stones of the series D_1 and D_2 are already stored outside for almost one year (D_1) and almost two years (D_2), respectively.

Samples, referred to as D_4, represent a material which is used to fill the open cavity of asphalt surfaces. It is a cementitious suspension consisting of cement, water, TiO_2, a fine sand fraction and possibly other ingredients. This slurry is applied on asphalt pavements and will fill the porosity which is connected to the surface. Directly after application, the slurry is present as a continuous layer. This layer will be removed within a short time, mainly depending on the traffic load and other parameters. Due to the polishing effect of the wheel load, the hardened material will be removed in layers. The asphalt matrix starts to appear again through the applied layer of slurry after a short time. At a certain moment, the asphalt matrix only bears all loads and therewith the removal rate of material slows down to marginal magnitudes. Hence, only a certain percentage of the total area can be considered to be an active surface. This should preferably also be the base for a comparative measurement. The producer of this product provided thin slabs, cast purely from this material. Therefore, the whole surface can be considered as active. Furthermore, the surface structure of this cast slabs shows distinct differences in roughness. As it is about slurry with only fine ingredients, the top side is plain and smooth whereas the backside shows a certain roughness. The latter case is assumed to more reliably represent the outside situation. Therefore, the undersurface was tested in regard to its NO_x degradation ability.

5.1.2. Results

In Fig. 5 the degradation of NO is given for every sample series. The graphs in Fig. 5 show the mean values of all measured samples out of one series (cp Table 4). Looking for the deviation of the measurements between different samples of one series it can be observed that there is no distinct variation.

The obtained measurement data show a wide spectrum of conversion rates. Samples of the series D_2 achieved the by far highest conversion rates and therewith have the highest air purification ability. Next, the series D_4 showed the second highest

Table 2
Tabular comparison of the patents owned by Mitsubishi Materials Corporation and Italcementi S.p.A.

	Mitsubishi Materials Corporation (Murata, 1997)	Italcementi S.p.A. (Cassar, 1997)
Name of the patent	NO_x-cleaning paving block	Paving tile comprising an hydraulic binder and photocatalyst particles
Field of the invention	NO_x-cleaning paving block with enhanced NO_x-cleaning capability due to an increased efficiency of fixing NO_x from the air and increased pluvial NO_x-cleaning efficiency and is provided with a non-slip property, wear resistance and decorative property.	- Hydraulic binder, dry premix, cement composition having improved property to maintain the brilliance and color quantity and to prevent esthetic degradation - Use of photocatalyst particles able to oxidize air and environmental pollutants
Working principle/ product requirements	- NO_x-cleaning paving block comprising a surface layer which contains TiO_2 and a concrete made base layer - NO_x-cleaning paving block with or without adsorbing material in the surface layer - Replacement of the sand used by 10–50% of glass grains or silica sand having a particle size of 1–6 mm - Surface layer having a void fraction of 10–40% and water permeability of 0.01 cm/s - NO_x-cleaning paving block roughened with a surface roughening tool	- Use of a photocatalyst which is able to oxidize in the presence of light air and environmental polluting substances for the preparation of an hydraulic binder for manufacturing paving tiles that maintain after installation for a longer time brilliance and color quantity - Use of a dry premix containing a hydraulic binder and a photocatalyst that is able to oxidize in the presence of light air and environmental polluting substances for manufacturing paving tiles that maintain after installation for a longer time brilliance and color quantity
Binder	- Cement	- Hydraulic binder - Cement (white, grey or pigmented) - Cement used for debris dams - Hydraulic lime
Photocatalyst	- TiO_2 without further requirements	- TiO_2 or a precursor thereof, mainly in the form of anatase - TiO_2 with anatase structure for at least 25, 50 and 70% - blend of anatase and rutile TiO_2 having a ratio 70:30 - TiO_2 doped with one or more atoms different from Ti - TiO_2 doped with one or more atoms selected from Fe(III), Mo(V), Ru(III), Os(III), Re(V), V(V), Rh(III) - Photocatalyst selected from the group consisting of tungstic oxide (WO_3), strontium titanate ($SrTiO_3$) and calcium titanate ($CaTiO_3$)
Amount of photocatalyst	- 0.6–20% by weight - 5–50% by weight with respect to the binder	- 0.01–10% by weight - 0.1% by weight with respect to the binder - 0.5% by weight with respect to the binder
Adsorbing materials	- Zeolite, magadiite, petalite and clay	- None
Thickness of the surface layer	- 2–15 mm	- Not given

results. Here, it has to be considered that for later application of this slurry seal the actual active surface will be reduced by the percentage of asphalt matrix. Series D_4 depicts only samples which are not representing the surface as it is in later application. For direct comparison, a sample of cut asphalt containing the slurry seal and being in service already for some time would have been required. With a notably lower conversion rate the series D_1 follows in this sequence. Finally, series D_3 only achieved low degradation rates. For this product it becomes questionable if the increased production expense and the likely higher market price can be justified by the slight air purification effect.

As mentioned earlier, a relation was found between the progress of the beginning conversion, maximum conversion rate and the decline of conversion during the measurement. For all samples it can be noticed that with higher maximum conversion the beginning conversion progresses faster and the decline becomes more apparent. However, the decline was approaching a constant degradation rate in all cases. This effect could be explained by an initial saturation of the reactive surface by reaction products and particularly by key precursors.

5.2. Influencing factors

The degradation of NO and therewith the performance of the photocatalytic reaction is governed by physicochemical as well as product related parameters. Hence, a short and descriptive explanation of the influencing factors irradiance, relative humidity, pollutant concentration and flow rate is given. The influence of the before mentioned parameters is investigated using sample D 2_2 used for the comparative tests on concrete paving blocks discussed in the previous section. The sample was carefully cleaned after each measuring cycle and dried at 105 °C for 24 hours. Besides varying experimental parameters, the influence of product related parameters like type of TiO_2 as well as content and application technique is investigated on self produced samples and will be addressed. Furthermore, the effect of red color pigments on the degradation rate was investigated and will be described as well. The remaining process conditions of the conducted measurements are based on the suggestions given in Sections 3 and 4 and kept constant at 50% relative humidity, 3 l/min flow rate, 1 ppmv pollutant concentration and 10 W/m^2 irradiance.

Table 3
Denomination and description of the tested photocatalytic concrete products.

Sample denomination	No. of samples	Type of sample	Description
D 1_1, D 1_2	2	Paving block	Taken from uncovered outside storage
D 2_1, D 2_2	2	Paving block	Taken from outside testing area
D 3_1 – D 3_3	3	Paving block	Samples withdrawn from production
D 4_1 – D 4_3	3	Asphalt slurry seal	Thin slab of cast pure slurry
D 5_1	1	Paving block	Samples withdrawn from production

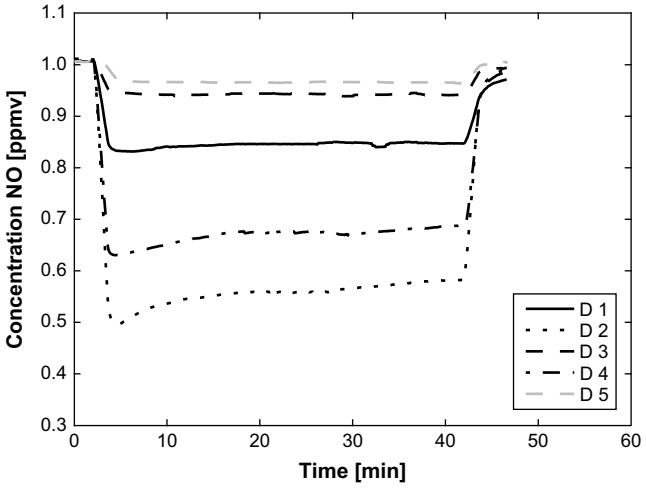

Fig. 5. Comparison of the degradation of nitric oxide (NO) over time for the tested concrete samples.

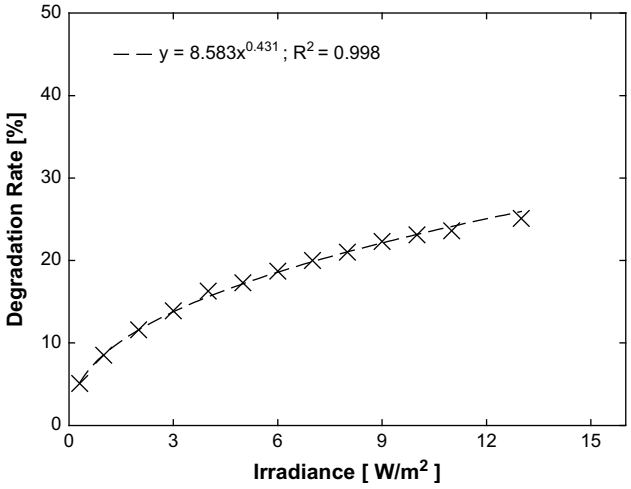

Fig. 6. Influence of the irradiance E on the degradation rate.

5.2.1. Process related parameters

5.2.1.1. Irradiance. The influence of the UV irradiance on the degradation rate is addressed before [9,16,20,21,22]. The degradation process of NO molecules is caused by the photocatalytic activity of TiO_2 in the anatase modification. The photocatalytic behavior of the catalyst results from the optoelectronic properties of this semiconductor. According to the explanation of the photocatalytic process given in Section 1, the UV-A light shows the most suitable range regarding the wavelength λ to start the PCO of undoped TiO_2. However, not only the wavelength is one of the influencing factors of the system's efficiency but also the intensity of the radiation or so-called irradiance E has an effect on the degradation rate.

According to Herrmann et al. [9], the increase of the photocatalytic activity, caused by an increase of the irradiance, can be divided into two regimes: i) for $E \leq 250\ W/m^2$ the degradation increases proportional to E and ii) for $E > 250\ W/m^2$ the photocatalytic activity grows with the square root of E. These two regimes are also reported by Lim et al. [16]. In contrast to Herrmann et al. [9], they give for the change over from first-order regime (linear behavior) to half-order regime (non-linear behavior) a value of above 10–20 W/m^2. The value for the change over from linear to non-linear behavior is defined by Obee and Brown [20] as one sun equivalent. An explanation of the two different regimes is given by Jacoby et al. [14]: the first-order regime where the electron-hole pairs are consumed more rapidly by the chemical reactions than by the recombination reaction which decrease the photocatalytic reaction rate; and the half-order regime where the recombination rate is dominant.

The linear behavior for values of low irradiance ($E < 15\ W/m^2$) could not be verified by own measurements. Fig. 6 shows the dependence of the NO removal on the irradiance for low values of irradiance based on own measurements on paving block D 2_2. A power function describes the relation between the irradiance E and achieved degradation rates for low values of irradiance ($E < 15\ W/m^2$). A linear behavior can only be assumed for values above 4 W/m^2. Due to the configuration of the light source of the setup, measurements using an irradiance of more than 15 W/m^2 could not be conducted.

According to Blöß and Elfenthal [2], the averaged UV-A irradiance of a cloudless summer midday amounts to approximately 35 W/m^2 for Central Europe. Furthermore, values in the range of 7–10 W/m^2 for the UV-A irradiance on cloudy days have been confirmed by own measurements. Additionally, an outside measurement was conducted with the same stone on a rainy day using the reactor cell described in Section 3. This test showed considerable results for the photocatalytic reaction and the dependency of the reaction on the UV-A irradiance (cp. Fig. 7). Based on these values and own observations, the functional capability of the photocatalytic reaction is ensured even for cloudy weather conditions with low values of UV-A irradiance.

5.2.1.2. Relative humidity. The influence of the relative humidity depends to a large extent on the type of material used. According to Beeldens [1], the hydrophilic effect at the surface prevails over the oxidizing effect when high values of relative humidity are applied.

Table 4
Degradation rates of the tested photocatalytic concrete products.

Sample	Degradation rate			Sample	Degradation rate		
	Deg_{beg}	Deg_{avg}	Deg_{end}		Deg_{beg}	Deg_{avg}	Deg_{end}
D 1_1	14.2	15.9	15.9	D 3_3	5.2	6.6	6.7
D 1_2	7.0	8.3	8.2	D 4_1 (coarse)	31.0	34.0	32.2
D 2_1	41.1	44.6	42.4	D 4_1 (fine)	2.1	2.8	2.7
D 2_2	37.6	41.3	38.7	D 4_2 (coarse)	32.4	33.5	30.9
D 3_1	5.0	6.6	6.6	D 4_3 (coarse)	32.3	37.7	36.4
D 3_2	5.2	6.6	6.5	D 5_8	2.5	4.0	4.1
D 1_1	14.2	15.9	15.9	D 3_3	5.2	6.6	6.7

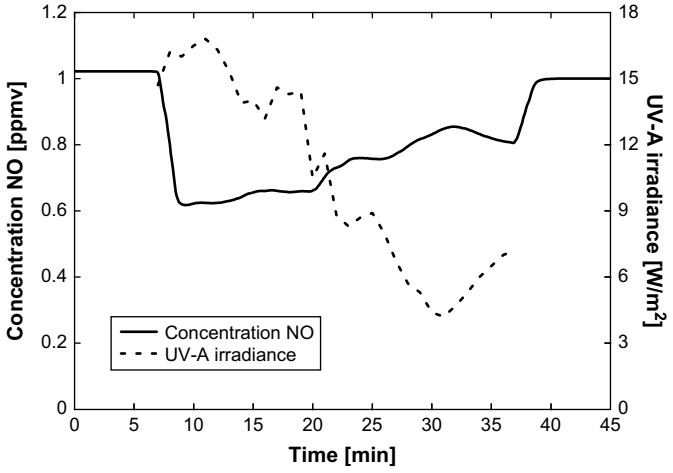

Fig. 7. Results of an outside measurement versus measured UV-A irradiance.

This is in line with findings for the application of self-cleaning glasses or anti-fogging glasses (cp. [8]). Here, no water droplets are formed as the photo-induced hydrophilicity of the surface forms a uniform thin layer of water. This thin water layer can either undergo pollutants which adhere to the surface or can prevent fogging of glasses. Due to the roughness of the concrete surface, the self-cleaning effect is not applicable to concrete surfaces in the same extent as for TiO_2 coated glass. Nevertheless, water molecules are adsorbed at the surface of the catalyst and therefore prevent the pollutant molecules to be adsorbed at the surface and further reactions with the TiO_2 will be hampered or not occur.

Fig. 8 gives an overview of the achieved degradation rates depending on the relative humidity, again using paving block D 2_2. It is evident from Fig. 8 that with increasing relative humidity the total efficiency of the system regarding the degradation of NO decreases linearly.

5.2.1.3. Pollutant concentration. The influence of the pollutant concentration on the NO degradation plays an important role when paving blocks are compared. Fig. 9 shows the influence of varying NO inlet concentrations on the achievable degradation rates for paving block D 2_2. It is obvious from Fig. 9 that increasing inlet concentrations result in lower degradation rates whereas lower pollutant concentrations are performance enhancing. Furthermore, changes of the pollutant concentration in the lower range result in remarkable higher changes of the degradation rate than changes in the range of higher concentrations. Therefore, also a limiting value for the degradation rate exists which will not fall short. This is also in line with observations reported by Herrmann et al. [9].

5.2.1.4. Flow rate. The flow rate or the therewith connected residence time of the pollutant molecules on the active surface of the concrete product can vary under practical conditions extensively as the wind speed as well as the wind direction is changing by time. Under laboratory conditions, various flow rates can be realized which result in different simulations of environmental conditions and therefore in unequal conditions for comparative tests. Fig. 9 shows the results for varying flow rates on the NO degradation of paving block D 2_2. High flow rates reduce the residence time of the pollutant molecules on the active surface, and hence the degradation rate is subsequently reduced, whereas lower flow rates enhance the degradation rate by a longer residence time of the model pollutant within the system.

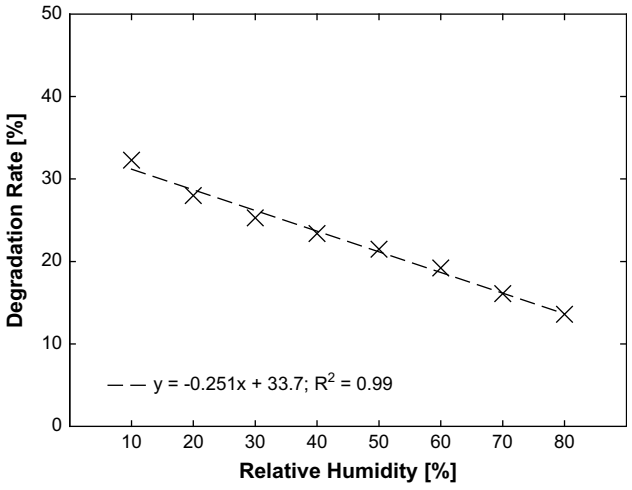

Fig. 8. Influence of the relative humidity on the degradation rate.

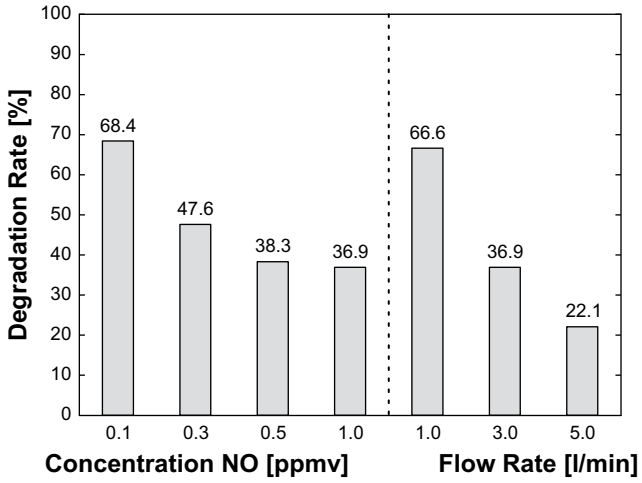

Fig. 9. Influence of the pollutant concentration and flow rate Q on the degradation rate.

5.2.2. Product related parameters

Not only changes of the physicochemical parameters of the test setup will influence the degradation of NO but also product related parameters are of great influence. Here, the type of TiO_2 as well as its content in the final product is relevant for the degradation process. Also the application method and a homogeneous distribution of the fine powder determine the efficiency of the final product. Furthermore, the influence of pigments is of great interest as a predominant part of the produced concrete paving blocks is sold with colored concrete.

5.2.2.1. Type of TiO_2 and application technique. Five different types of TiO_2 were selected for self-developed mortar samples (Table 5). The selected powders cover four commercially available standard TiO_2 in the anatase modification (TiO_2 A–D) as well as one carbon-doped TiO_2 (TiO_2 E) of which the particle size distribution (PSD) is comparable to the PSD of the undoped powder acting in the UV-A range (TiO_2 D).

Test mortars containing 3%, 5% and 10% TiO_2 were produced. The mix design of the composed mortars is given in Table 6. The TiO_2 content is based on the binder mass of the reference mortar which is chosen to be equal for all tested powders.

Besides varying powder contents, the application technique of the powder was changed during the experiments. Applying the TiO_2 as dry powder or water based suspension was suitable for the experiments in the lab. The dry powder was added combined with the binder whereas the suspension was added with the mixing water. Furthermore, the influence of different surface conditions is

Table 5
Properties of the deployed TiO_2.

	TiO_2 A	TiO_2 B	TiO_2 C	TiO_2 D	TiO_2 E[a]
Specific density [g/cm^3]	3.9[b]	3.94	3.9	3.9[b]	3.9[b]
Characteristic particle size [μm]					
$d_{0.1}$	0.65[c]	1.193	0.641[c]	0.593[c]	0.574[c]
$d_{0.5}$	1.245[c]	2.72	2.104[c]	2.014[c]	2.075[c]
$d_{0.9}$	2.487[c]	6.535	7.123[c]	4.349[c]	4.92[c]
Computed surface area					
Specific surface [cm^2/g]	15 847[c]	7916	11,910[c]	13,139[c]	13,113[c]
Specific surface [m^2/cm^3]	6181[c]	3115	4645[c]	5195[c]	5114[c]

[a] Carbon-doped TiO_2.
[b] Value taken from data sheet.
[c] Based on measured agglomerates.

Table 6
Mortar composition.

	Reference mortar		3% TiO_2	5% TiO_2	10% TiO_2
	[dm^3/m^3]	[kg/m^3]	[kg/m^3]	[kg/m^3]	[kg/m^3]
CEM I 52.5N	195.8	600.0	600.0	600.0	600.0
Sand 0-2	490.6	1300.0	1300.0	1300.0	1300.0
TiO_2	–	–	18	30	60
Water	250.0	250.0	250.0	250.0	250.0

considered by different treatments of the bottom and top side of the produced slabs. The bottom side of the hardened slabs was sandblasted in order to remove a covering cement layer from the TiO_2 particles and to roughen this side. The top side of the slabs was ground to equalize this surface. Furthermore, it is assumed that on the ground side of the samples equal test conditions can be achieved as the TiO_2 is equally distributed within the sample and not covered by a cement layer. The produced and pretreated concrete slabs were tested on the ground surface according to the procedure described in Section 4.

In Fig. 10 the results for all samples containing the 3% suspension of TiO_2 are shown. The experimental data show a clear dependence on the fineness of the powder (cp. Fig. 10 and Table 5). This is in line with the expectations caused by the higher specific surface area of e. g. TiO_2 C, which is about 30% higher than the surface area of TiO_2 B. Furthermore, the effectiveness of the degradation of NO could be increased for the doped TiO_2 E as this modified powder uses UV-A radiation as well as bigger parts of the visible light. In Fig. 11 the results of the sandblasted surface for TiO_2 B are shown for varying powder contents and application methods. The test results clearly show that with increasing powder content the degradation rate also increases.

Furthermore, it is obvious from Fig. 11 that higher conversion rates can be obtained when the powder is applied as suspension. The advantage of a better distribution of the powder can be shown by the higher conversion rates of the slabs containing 3% and 5% TiO_2 as suspension. Here, applying the powder as suspension added to the mixing water allows a better and more homogeneous distribution of the powder. The degradation of NO in dependence on the light source for a doped TiO_2 powder is shown in Fig. 12. In comparison with Fig. 10, the doped TiO_2 E shows a better performance as the undoped TiO_2 D.

Although the contribution in the visible light spectrum (measuring range of the VIS-L sensor 500–640 nm) is marginal, the

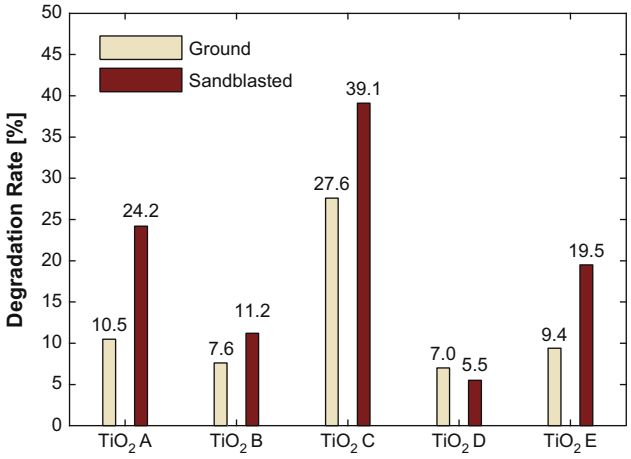

Fig. 10. Influence of the powder used on the degradation rate.

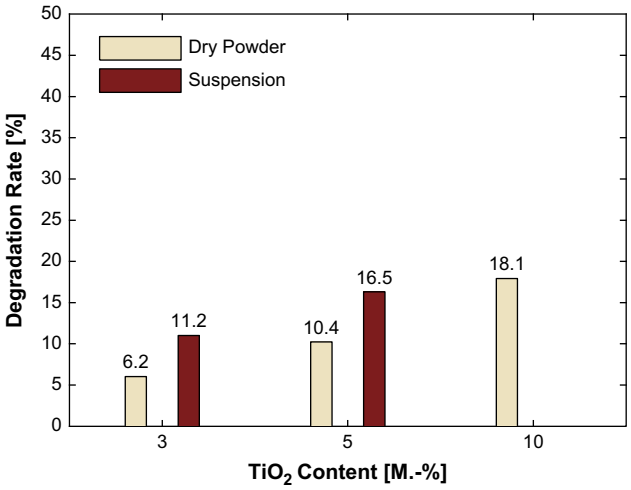

Fig. 11. Influence of the application technique of the TiO_2 on the degradation rate.

UV-A radiation is used more efficiently in the higher UV-A range ($\lambda > 380$ nm) and the lower visible light range ($\lambda > 500$ nm) as the relative photocatalytic activity is enhanced in this range [2] and increases the overall performance of the TiO_2 E.

5.2.2.2. Influence of pigments. Enhanced esthetic and architectural requirements in inner-city areas on the paving of public places demand the application of colored concrete paving blocks. The application of pigments helps to integrate a concrete paving within an already existing architectural situation. This meets the public perceptions regarding the esthetic quality of public places, but it may cause also problems when photocatalytic materials are applied. Problems mainly result from an increased water demand of the mixtures when fine pigment particles are added.

For a demonstration project in the Dutch city of Hengelo, approximately 1000 m^2 of classical paving will be replaced by photocatalytic active concrete paving blocks. Therefore, the influence of two different red pigments on the degradation process of photocatalytic paving blocks was investigated. The results of the test carried out in the lab are incorporated in the production of the concrete paving blocks used for the demonstration project. The main results of this investigation are depicted in Fig. 13. The direct

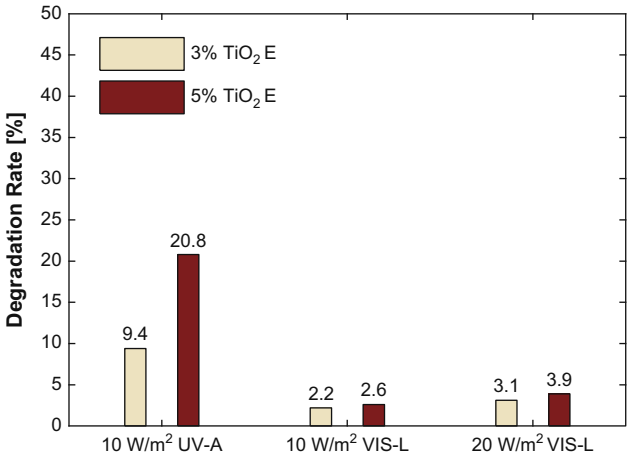

Fig. 12. Influence of the applied light source on the degradation rate of carbon-doped TiO_2.

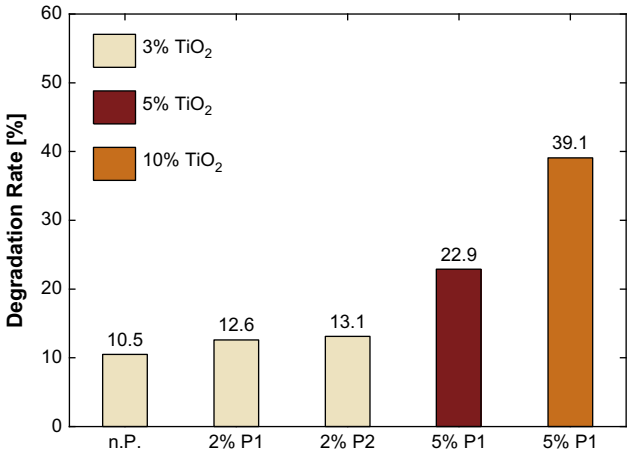

Fig. 13. Influence of red pigments on the degradation rate: no pigment (n.P.); 2% pigment type 1 (2% P1); 2% pigment type 2 (2% P2); 5% pigment type 1 (5% P1).

comparison shows that the degradation rate of the mix containing 3% TiO_2 (no pigment, 2% P1, and 2% P2) is not influenced by the added pigments. The values of the degradation rates are varying in the same order of magnitude as expected for the scattering of the measuring data. Also, higher contents of TiO_2 (5% and 10%) associated with higher pigment contents (5% P1) are not reducing the degradation rates verifiably. Solely the workability of the fresh concrete mix was reduced significantly as the content of fine particles (TiO_2 and red pigment) was increased.

6. Conclusions

This paper addresses the properties and the evaluation of air-purifying properties of concrete products containing photocatalytic active titanium dioxide (TiO_2). Both commercial products and self-developed mortars were tested. For evaluating the air-purifying abilities of these concrete products, a suitable test setup was developed which is based on the degradation of nitric oxide (NO) described in the standard ISO 22197-1:2007. By means of the setup, the influencing parameters on the degradation process of NO are investigated. With respect to the number of influencing parameters and their partial major influence on the measurement it is advisable to agree a common test standard using equal boundary conditions. Based on these findings as well as specifications in the literature and standards, a suitable test procedure for the evaluation of concrete paving blocks is suggested.

Using the described test procedure, a comparative study on cementitious products was carried out in order to assess the efficiency of different products available on the European market. It can be noticed that the European market provides a variety of products, showing air-purifying abilities. However, their efficiency in regard to NO degradation was found to vary in a notable scale. There are products achieving mean degradation rates of about 40% under the above described optimum laboratory conditions, whereas other products almost show no or an insignificant effect. Hence, the assessment of concrete products for projected constructions becomes more difficult for the planning engineer as the total conversion of large areas can be influenced notably by the selection of the paving blocks. With the proper selection of air-purifying products a contribution for the environment and an active remedy for atmospheric pollution can effectively be achieved. For large areas like parking lots or broad sidewalks and bicycle lanes, in particular the total conversion can be influenced notably by the selection of the paving stones.

Furthermore, the effect of varying experimental parameters on the degradation process was studied. Therefore, one concrete paving block used for the comparative study was extensively tested under varying experimental parameters to investigate the influence of physicochemical parameters. For investigating the effect of product related parameters, also new mortar mixes with different types of TiO_2 are designed and tested regarding their NO degradation efficiency. Regarding physicochemical parameters and product related parameters it can be concluded that:

1. An increase of the irradiance in the range of the cut-off wavelength of the applied photocatalyst is increasing the degradation performance of the product.
2. Increasing relative humidity values are reducing the degradation rate of the photocatalytic concrete product as the water molecules compete with the pollutant molecules at the active surface of the photocatalyst.
3. Increasing pollutant concentrations are resulting in higher conversion rates up to a limiting value whereas the overall degradation rate is decreasing.
4. High flow rates are reducing the residence time of the pollutant molecules on the concrete surface and therefore the degradation rate is reduced.
5. Higher amounts of TiO_2 are enhancing the performance of the products regarding NO degradation.
6. The application of finer TiO_2 is showing a bigger effect on the degradation rate than higher amounts of TiO_2.
7. The surface structure was, in this respect, found to have a major influence as well. Surfaces with high roughness are providing more active surface area than smooth surfaces.
8. The application of TiO_2 suspensions showed good results regarding a more homogeneous distribution of the powder. Therefore, the efficiency of the photocatalytic concrete product can be enhanced when the photocatalyst is applied as suspension and not as dry powder as usual.
9. The combination of red color pigments and TiO_2 did not showed an explicit influence on the degradation rate.

Furthermore, more fundamental research on the influencing factors is necessary to reliably model the degradation process. Here, especially long term experiments for the evaluation of the duration and durability of the NO degradation process are of special interest. The presented results are used for establishing an appropriate reaction model as basis for the modeling of later outdoor measurements of the degradation process as well as its influencing parameters. Relations have to be established in the model between laboratory results and real scale outdoor application of these concrete products.

Finally, the current patent situation makes it difficult to enter the market with new ideas without breaching existing patent rights. One of the promising opportunities would be the expansion of the degrading effect from the active surface into deeper layers of the top layer by means of e.g. UV-A transmitting glass particles and surface layers having a porous structure.

Acknowledgements

The authors wish to express their sincere thanks to the European Commission (I-Stone Project, Proposal No. 515762-2) and the following sponsors of the research group: Bouwdienst Rijkswaterstaat, Rokramix, Betoncentrale Twenthe, Graniet-Import Benelux, Kijlstra Beton, Struyk Verwo Groep, Hülskens, Insulinde, Dusseldorp Groep, Eerland Recycling, ENCI, Provincie Overijssel, Rijkswaterstaat Directie Zeeland, A&G maasvlakte, BTE, Alvon

Bouwsystemen, and v. d. Bosch Beton (chronological order of joining).

Appendix. List of symbols

Roman

B	width [mm]
$C_{g,in}$	inlet concentration [ppmv]
Con	conversion [ppmv]
D_h	hydraulic diameter [m]
Deg	degradation rate [%]
E	irradiance [W/m^2]
E_g	band gap energy [eV]
e^-	electron
f	frequency [Hz]
h	Planck's constant [eVs]
h^+	electron hole
H	slit height [mm]
L	length [mm]
L_d	critical length [mm]
Q	flow rate [l/min]
Re	Reynolds number [-]
t	time interval [s]
v	fluid velocity [m/s]

Greek

λ	wavelength [nm]
μ_{air}	dynamic viscosity [Ns/m^2]
υ_{air}	kinematic viscosity [m^2/s]

Subscript

air	Air
avg	Average
beg	Begin
end	End
tot	total

References

[1] Beeldens A. Air purification by road materials: results of the test project in Antwerp. In: Baglioni P, Cassar L, editors. Proceedings international RILEM symposium on photocatalysis, environment and construction materials, 8–9 October 2007, Florence, Italy. Bagneux, France: RILEM Publications; 2007. p. 187–94.

[2] Blöß SP, Elfenthal L. Doped titanium dioxide as a photocatalyst for UV and visible light. In: Baglioni P, Cassar L, editors. Proceedings international RILEM symposium on photocatalysis, environment and construction materials 8–9 October 2007, Florence, Italy. Bagneux, France: RILEM Publications; 2007. p. 31–8.

[3] Burmeister LC. Convective heat transfer. John Wiley and Sons Inc.; 1993.

[4] Cassar L, Pepe C. Paving tile comprising an hydraulic binder and photocatalyst particles. EP-patent 1 600 430 A1, Italcementi S.p.A., Italy; 1997.

[5] Council Directive 1999/30/EC. Relating to limit values for sulphur dioxide, nitrogen dioxide and oxides of nitrogen, particulate matter and lead in ambient air. Official Journal of the European Communities 1999.

[6] Dalton JS, Janes PA, Jones NG, Nicholson JA, Hallam KR, Allen GC. Photocatalytic oxidation of NO_x gases using TiO_2: a surface spectroscopic approach. Environmental Pollution 2002;120(2):415–22. doi:10.1016/S0269-7491(02)00107-0.

[7] Directive 2001/81/EC of the European Parliament and of the Council on national emission ceilings for certain atmospheric pollutants. Official Journal of the European Communities 2001. L 309/22–30.

[8] Hashimoto K. TiO_2 photocatalysts towards novel building materials. In: Baglioni P, Cassar L, editors. Proceedings international RILEM symposium on photocatalysis, environment and construction materials, 8–9 October 2007, Florence, Italy. Bagneux, France: RILEM Publications; 2007. p. 3–8.

[9] Herrmann JM, Péruchon L, Puzenat E, Guillard C. Photocatalysis: from fundamentals to self-cleaning glass application. In: Baglioni P, Cassar L, editors. Proceedings international RILEM symposium on photocatalysis, environment and construction materials, 8–9 October 2007, Florence, Italy. Bagneux, France: RILEM Publications; 2007. p. 41–8.

[11] Horiba Ltd. Operations manual – ambient NO_x monitor APNA-360, 3rd ed.; April 1998.

[12] ISO 22197-1:2007. Fine ceramics (advanced ceramics, advanced technical ceramics) – test method for air-purification performance of semiconducting photocatalytic materials – part 1: removal of nitric oxide; 2007.

[13] ISO 7996:1985. Ambient air – determination of the mass concentration of nitrogen oxides – chemiluminescence method; 1985.

[14] Jacoby WA, Blake DM, Noble RD, Koval CA. Kinetics of the oxidation of trichloroethylene in air via heterogeneous photocatalysis. Journal of Catalysis 1995;157(1):87–96. doi:10.1006/jcat.1995.1270.

[15] Lahl U, Lambrecht U. High NO_2 levels: ongoing need for action on diesel emissions. In: Technical congress 2008. Verband der Automobilindustrie; 2008.

[16] Lim TH, Jeong SM, Kim SD, Gyenis J. Photocatalytic decomposition of NO by TiO_2 particles. Journal of Photochemistry and Photobiology A: Chemistry 2000;134(3):209–17. doi:10.1016/S1010-6030(00)00265-3.

[17] Liu CC, Hsieh YH, Lai PF, Li CH, Kao CL. Photodegradation treatment of azo dye wastewater by UV/TiO_2 process. Dyes and Pigments 2006;68(2–3):191–5. doi:10.1016/j.dyepig.2004.12.002.

[18] Matsuda S, Hatano H, Tsutsumi A. Ultrafine particle fluidization and its application to photocatalytic NO_x treatment. Chemical Engineering Journal 2001;82(1-3):183–8. doi:10.1016/S1385-8947(00)00339-9.

[19] Murata Y, Tawara H, Obata H, Murata K. NO_X-cleaning paving block. EP-patent 0 786 283 A1. Mitsubishi Materials Corporation, Japan; 1997.

[20] Obee TN, Brown RT. TiO_2 photocatalysis for indoor air applications: effects of humidity and trace contaminant levels on the oxidation rates of formaldehyde, toluene, and 1,3-butadiene. Environmental Science and Technology 1995;29(5):1223–31. doi:10.1021/es00005a014.

[21] Ollis DF, Pelizetti E, Serpone N. Photocatalyzed destruction of water contaminants. Environmental Science and Technology 1991;25(9):1523–9. doi:10.1021/es00021a001.

[22] Peral J, Ollis DF. Heterogeneous photocatalytic oxidation of gas-phase organics for air purification: acetone, 1-butanol, butyraldehyde, formaldehyde, and *m*-xylene oxidation. Journal of Catalysis 1991;136(2):554–65. doi:10.1016/0021-9517(92)90085-V.

[23] Rajeshwar K, Chenthamarakshan CR, Goeringer S, Djukic M. Titania-based heterogeneous photocatalysis – materials, mechanistic issues, and implications for environmental remediation. Pure and Applied Chemistry 2001;73(12):1849–60. doi:10.1351/pac200173121849.

[24] Stephan D, Wilhelm P, Schmidt M. Photocatalytic degradation of rhodamine B on building materials – influence of substrate and environment. In: Baglioni P, Cassar L, editors. Proceedings international RILEM symposium on photocatalysis, environment and construction materials, 8–9 October 2007, Florence, Italy. Bagneux, France: RILEM Publications; 2007. p. 299–306.

[25] VROM. Traffic emissions policy document – achieving sustainability through cleaner, more efficient and quieter vehicles, and climate-neutral fuels. The Netherlands Ministry of Housing, Spatial Planning and the Environment; 2004.

[26] Wang HQ, Wu ZB, Zhao WR, Guan BH. Photocatalytic oxidation of nitrogen oxides using TiO_2 loading on woven glass fabric. Chemosphere 2007;66(1):185–90. doi:10.1016/j.chemosphere.2006.04.071.

[27] Zhao J, Yang XD. Photocatalytic oxidation for indoor air purification: a literature review. Building and Environment 2003;38(5):645–54. doi:10.1016/S0360-1323(02)00212-3.